Catalysis Today 157 (2010) 170–176

Contents lists available at ScienceDirect

Catalysis Today

journal homepage: www.elsevier.com/locate/cattod

The deposition of coke during carbon dioxide reforming of methane over intermetallides

Larisa A. Arkatova*

Department of Chemistry, Tomsk State University, Lenin Av. 36, 634050 Tomsk, Russia

ARTICLE INFO

Article history:
Available online 3 April 2010

Keywords:
CH_4–CO_2 reforming
Intermetallides
Synthesis gas
Carbon deposition
Filaments

ABSTRACT

Dry reforming of methane was studied over the systems on the base of Ni_3Al and Ni_3Al + 5%Mo in the temperature range 600–900 °C. The materials have been prepared by self-propagating high temperature synthesis and characterized by XRD (in situ and ex situ), DTA–TG, SEM + EDX, HRTEM + EDS and XPS. The formation of Mo_2C phase was observed at moderate Mo content (5–10 wt.%), which corresponds to a much improved catalytic activity and stability under the severe carbon dioxide reforming conditions. The structure and morphology of different types of carbon deposits obtained on Ni_3Al and Ni_3Al + 5%Mo catalysts were investigated. The results indicated that the addition a low amount of Mo to Ni_3Al led to a decrease in carbon deposition. It is shown that Ni_3Al + 5%Mo is promising catalyst for dry reforming of methane with carbon dioxide.

1. Introduction

Carbon dioxide reforming of methane, i.e. dry reforming of methane (DRM), has received considerable attention as a promising way that enables the utilization of natural gas and reduction of greenhouse gases [1–3]. DRM is one of the processes to produce synthesis gas with desired H_2/CO ratio for clean fuels and chemicals [4–12]. The low H_2/CO ratio is preferentially used for the production of liquid hydrocarbons (Fischer–Tropsch synthesis), formaldehyde and polycarbonates [4]. This reaction has also been suggested as a candidate for solar energy storage [4], as a method of recovering excess heat from gas turbine exhaust [5], and as a source of CO and H_2 for flame stabilization in low temperature methane fired gas turbines [6].

Three basic reactions may be used to convert natural gas to syngas (CO + H_2):

steam reforming of methane (SRM):

$$CH_4 + H_2O = CO + 3H_2, \quad \Delta H = 206.3\,\text{kJ/mol} \tag{1}$$

carbon dioxide reforming of methane, or dry reforming of methane:

$$CH_4 + CO_2 = 2CO + 2H_2, \quad \Delta H = 247.3\,\text{kJ/mol} \tag{2}$$

partial oxidation of methane (POM):

$$CH_4 + (1/2)O_2 = CO + 2H_2, \quad \Delta H = -35.6\,\text{kJ/mol} \tag{3}$$

Among these three processes, only SRM has been industrialized, although the other processes may also have certain advantages [10–12].

Ni-based catalysts, the traditional catalysts for SRM, are widely used for DRM as well because of high activity and low cost. However, a rapid deactivation due to carbon deposition and/or sintering of the metal particles has been reported on Ni/oxidic support catalysts [7,8]. There is a general agreement about noble metals showing a better activity and lower degree of carbon deposition [7,13]. Most authors preferred Rh, Pt [14–16]. van Keulen et al. [15] showed that Pt is one of the most active and stable metals among zirconia supported group VIII metals and Pt/ZrO_2 has a very high feedstock of CH_4/CO_2 = 2. Choudhary et al. [17] found that nickel supported on silica and/or alumina pre-coated with MgO, CaO or rare earth oxides showed much higher activity, selectivity and productivity in the methane-to-syngas conversion process than the catalysts prepared using supports without any precoating. Further study of Choudhary et al. [18] showed that the best performance was shown by MgO among the precoating metal oxides. Mehr et al. [19] studied the influence of MgO in the DRM to syngas, and found that addition of MgO reduced the carbon deposition and energy consumption. MgO-promoted catalysts are resistant to coking due to Lewis basicity of MgO [19–21].

DRM is accompanied by very unfavorable and undesired formation of different kinds of carbon deposits [22,23], particularly a filamentary carbonaceous deposits, which, by mechanically

* Tel.: +7 3822473449; fax: +7 3822529895.
E-mail address: larisa-arkatova@yandex.ru.

0920-5861/$ – see front matter © 2010 Elsevier B.V. All rights reserved.
doi:10.1016/j.cattod.2010.03.003

destroying the catalyst, can make its deactivation irreversible. Therefore, one of the most important properties of a good catalyst for DRM is its resistance to coking [24,25]. Some authors tried to solve this problem by introduction of certain additions in catalysts [26–29].

This work focuses on a novel synthetic approach based on the self-propagating high-temperature synthesis (SHS) which can be applied successfully to preparing Ni_3Al, containing Ni phase [30,31]. SHS is based on rapid, highly exothermic solid flame reactions between powders to produce very high temperatures and stable products containing a high concentration of structural defects which can act as the active sites in heterogeneous catalysis.

Ni_3Al intermetallic compound is known as a promising high temperature material because of its excellent high temperature strength and good corrosion/oxidation resistance [32]. But no promising catalytic properties have been reported for this compound. The catalytic group [33] found that Ni_3Al, in the form of both powder and foil exhibits high catalytic activity for methanol decomposition and SRM.

Taking into consideration some advantages of intermetallides (resistance in aggressive oxidizing atmospheres; high thermoresistance; stability, mechanical tics; and thermal conductivity) and also high activity and stability of Mo_2C as the catalyst for DRM [24,34,35], the aim of the present work was to realize an idea of forming some active phases on the base of Mo_2C and metallic Ni on Ni_3Al surface directly in the reactor. It was demonstrated that such a novel synthetic approach can successfully be applied to preparing intermetallides. It will also be shown that the process of catalyst preparation can substantially be shortened in time, as the active components such as Ni and Mo_2C can be formed *in situ* – inside a catalytic reactor – under the DRM reaction atmosphere upon increasing temperature without any separate stages of labor- and time-consuming Mo_2C synthesis. Another purpose of this study was to investigate the structure and properties of carbon deposited on the surface of Ni_3Al and Ni_3Al + 5%Mo during CO_2–CH_4 reforming.

2. Experimental

2.1. Catalyst preparation

Intermetallides were synthesized by the method of self-propagating high temperature synthesis (SHS) from the powders of Ni (Nornickel), Al (SUAL-PM, Shelekhov) and Mo (TU 48-19316-92, MOLIDEX-M) which were preliminarily dried in vacuum at temperature 100 °C for 3 h. The powders were not specifically treated (for example, in H_2 atmosphere) due to the following reasons: (1) the original powders were obtained by electroplating technique, (2) H_2 is unfavourable for combustion kinetics [36], (3) undesirable-obtaining of metal hydrates at high SHS temperatures (1100–1200 °C) [36]. A half-finished products of cylindrical shape were prepared from the prepared mixtures of powders by the method of double-action pressing using a bench press with dismountable die mold and floating piston. SHS of pressed samples were conducted in the bomb with constant pressure in argon atmosphere. Heat impulse was supplied to a butt part of the pressed intermediates using a W-spiral. Thus chemical reaction is ignited and spreaded spontaneously as wave transmission along the axis of pressed intermediates. Then derived samples in the shape of bar were crushed and sifted. Fractions with the size of 400–600 μm were tested in the catalytic set-up.

2.2. Catalyst characterization

The X-ray diffraction patterns were measured before and after catalytic experiments at room temperature using diffractometer Shimadzu XRD-6000 (Japan) (Cu Ka radiation, λ = 0.154187 nm). Database: PCPDFWIN and POWDER CELL 2.4. *In situ* XRD experiments were carried out in the VEPP-3 station of Siberian Synchrotron and Terahertz Radiation Center of Budker Institute of Nuclear Physics of SB RAS. Morphology of catalysts was investigated using scanning electron high-vacuum microscope VEGAII LMU (Czech Republic) coupled with an X-ray energy-dispersive spectroscopy (EDS) system (Oxford INCA Energy 350). The surface areas (BET) were determined by nitrogen adsorption using an automated gas adsorption analyzer (ChemiSorb 2750, Micromeritics, USA) linked with mass-spectrometer QMS-300 (Stanford Research System, USA). Thermogravimetry–differential thermal analysis (DTA–TG) measurements were conducted under oxidative (20 $cm^3\,min^{-1}$) atmosphere with STA 409 Luxx (NETZSCH, Germany) using 30–50 mg of samples and a 10 °C min^{-1} increase rate from room temperature to 1000 °C. Transmission electron microscopy (TEM) was performed with JEOL JEM-2010 machine equipped with Gatan slow-scan camera for high-resolution observation and energy-dispersive X-ray microanalyzer (EDX) for elemental analysis of specimen surface. The accelerating voltage applied was 200 kV.

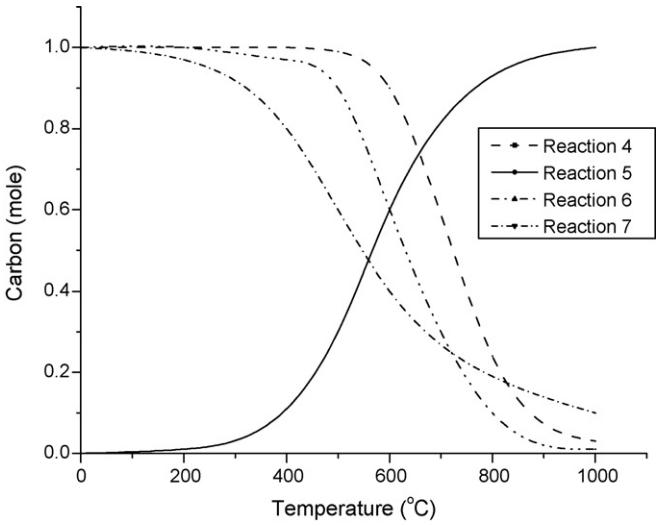

Fig. 1. Coke formation via reactions (4)–(7) as a function of temperature.

2.3. Catalytic tests

Catalytic activity was investigated in a temperature-programmable quartz tube reactor with inner diameter of 5 mm and a length of 150 mm in conditions: temperature range 600–900 °C, space velocity of gas stream 100 cm^3/min and molar ratio CO_2:CH_4 = 1:1. The vertically mounted reactor was charged with a catalyst (400–600 μm), and the reaction gases (CH_4–CO_2–He 20:20:60 $cm^3\,min^{-1}$) were introduced with upstream flow direction. Then reactor was heated to required temperature (for example, 900 °C) with 10 °C min^{-1} rate. When the temperature approached the value, the sampling of post-reactor gas phase

Table 1
BET surface areas of Ni_3Al and Ni_3Al + 5%Mo catalysts before and after 24-h DRM reaction.

Catalysts	Before reaction ($m^2\,g^{-1}$)	After 24-h reaction ($m^2\,g^{-1}$)			
		600	700	800	900
Ni_3Al	1.2	1.1	0.9	0.7	0.6
Ni_3Al + 5%Mo	1.3	1.3	1.1	0.9	0.8

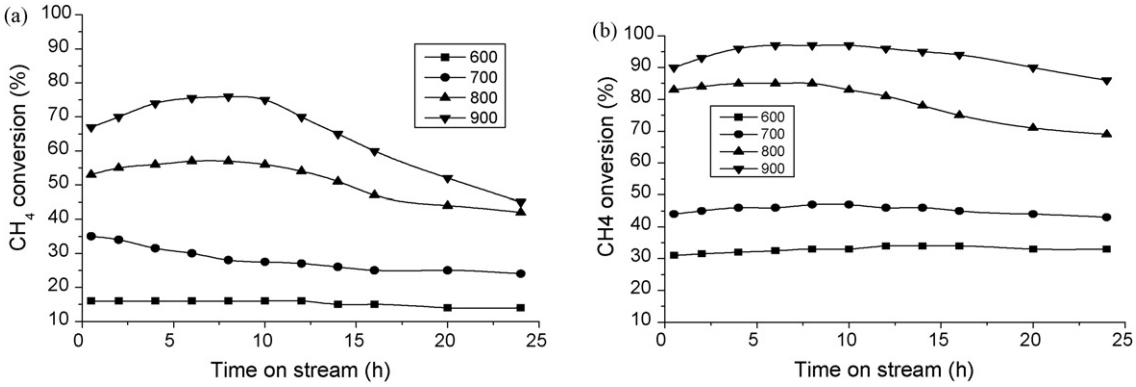

Fig. 2. CH_4 conversion during DRM over Ni_3Al (a) and Ni_3Al + 5%Mo (b) at 600, 700, 800, and 900 °C as a function of reaction time.

was started. Analysis of reaction products was carried out by gas chromatography (GC) using Carbosieve SII and Porapak Q packed columns. After 24 h time on stream at 900 °C admission of methane and carbon dioxide was stopped, and the reactor was cooled to room temperature under flow of He. The conversion was calculated on the basis of the feed flow rates and the dry exit gas composition as obtained by GC. Exhaust gases were analyzed using a TCD.

3. Results and discussions

3.1. Coke formation boundary

The formation of coke during the catalytic dry reforming could lead to a deactivation of catalysts, resulting in low durability and activity. Thus it is important to keep it under control. The most probable reactions [34] leading to carbon formation are listed below:

$$2CO = CO_2 + C \quad \text{(Boudouard reaction)} \tag{4}$$

$$CH_4 = 2H_2 + C \quad \text{(Methane thermolysis)} \tag{5}$$

$$CO + H_2 = H_2O + C \tag{6}$$

$$CO_2 + 2H_2 = 2H_2O + C \tag{7}$$

Fig. 1 shows the carbon formation as a function of temperature via each reaction [29]. This is to determine the role of each reaction on carbon formation thermodynamically.

Reactions (4), (6) and (7) are not significant in coke formation at high temperature, while reaction (5) is favorable. It is well known that by increasing the H:C ratio in the reactor feed, the coke formation rate will decrease due to a shift in the equilibrium of reaction (5).

3.2. Methane conversion

The catalytic performances of Ni_3Al and Ni_3Al + 5%Mo for DRM were investigated at temperatures 600, 700, 800, and 900 °C for 24 h. The CH_4 conversion is plotted as a function of reaction time, as shown in Fig. 2. It was defined the value after the first 0.5 h reaction as the "initial conversion" because of the necessity to overcome the initial nonequilibrium state. As we previously reported in the isochronal tests [31,32], the initial conversion rapidly increases with temperature and reaches a maximum of 79% and 99% at 900 °C for Ni_3Al and Ni_3Al + 5%Mo, respectively. The variation in the CH_4 conversions with time strongly depends on the reaction temperature.

At 600 °C, the conversions remain stable over time, showing no considerable change after 24 h, although they are low, about 18 and 30% for Ni_3Al and Ni_3Al + 5%Mo, respectively. At 700 °C, the conversions slightly decrease with time. In contrast, at first the conversions increase slowly during 3–4 h and then they remain constant, and after 10–12 h at 800 °C they begin to decrease slowly. Thus, it turns out that the activity and stability of these two catalysts are different: Ni_3Al + 5%Mo is more active and stable than Ni_3Al.

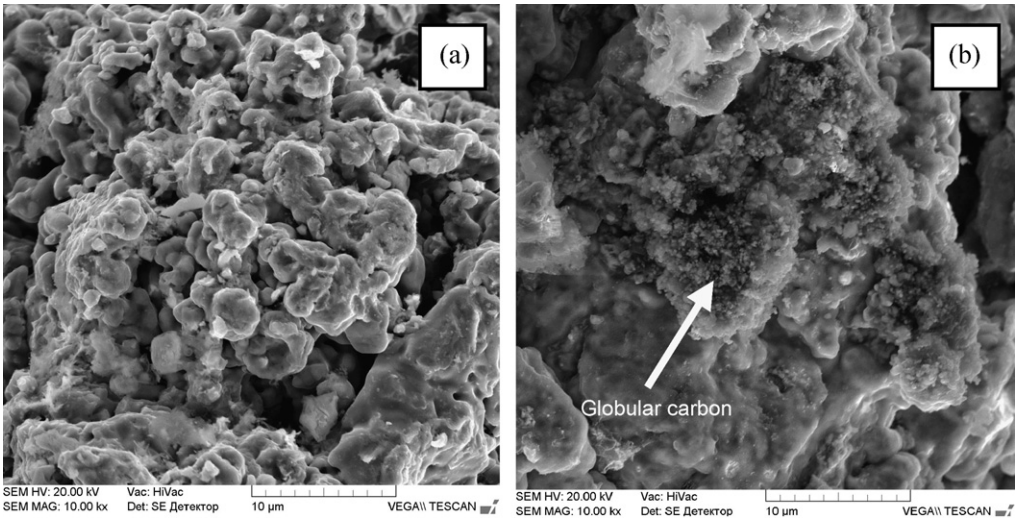

Fig. 3. SEM micrographs of Ni_3Al catalysts: (a) initial sample, (b) after DRM. (Time on stream 24 h, T = 600–950 °C, $V(CO_2:CH_4)$ = 100 cm^3/min, $CO_2:CH_4$ = 1:1).

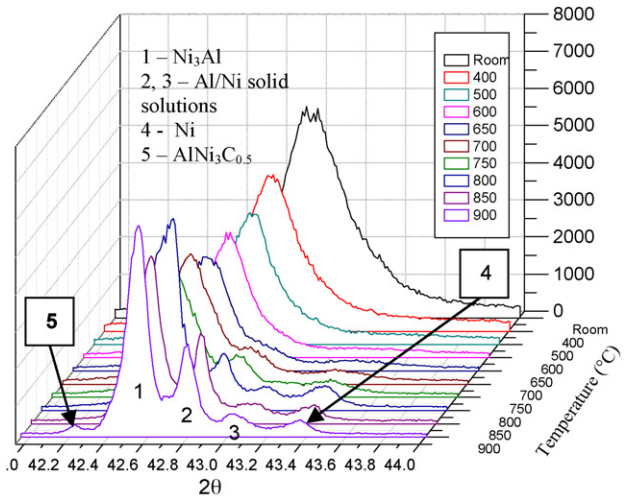

Fig. 4. *In situ* XRD patterns of Ni_3Al catalyst before catalytic test at room temperature (black pattern) and during DRM with increasing temperature from 400 to 900 °C with molar CO_2:CH_4 ratio equal 1:1. Fragment (2θ = 42–44°).

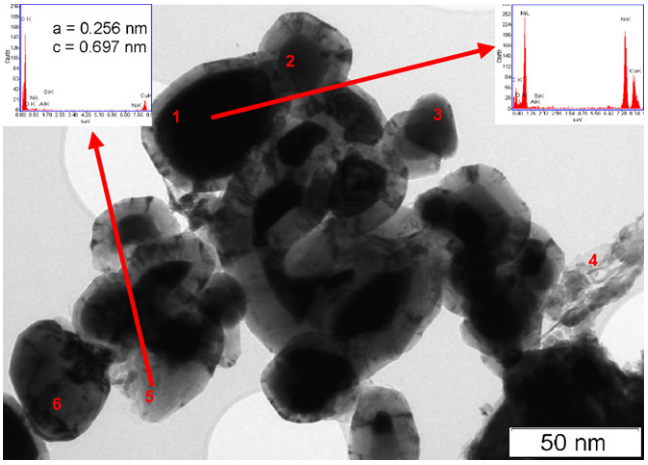

Fig. 5. TEM bright field image of Ni_3Al surface after reaction for 24 h at 900 °C. EDS spectra taken from position 1, showing the presence of Ni particles, EDS spectra taken from position 5, showing the formation graphite phase on the catalyst surface.

3.3. Surface characterization

The BET surface areas of the intermetallides before and after 24-h reaction are listed in Table 1. Initial surface areas were small enough, for example, 1.2 $m^2\,g^{-1}$ for Ni_3Al and 1.3 $m^2\,g^{-1}$ Ni_3Al + 5%Mo. The surface areas decreased slightly after reaction at 600 °C. At higher temperature above 800 °C, the surface area decreased significantly to approximately one-quarter.

The SEM morphologies of Ni_3Al surface before and after DRM are shown in Fig. 3. The surface is rough and porous before reaction. The fine nickel particles exist on the surface, though they are not visible in the SEM observation. But we observed a change in the morphology of globular structure after the DRM tests. On some parts of Ni_3Al surface we can observe globular "caps", covering 20–30% of the surface. The most likely, it depends on the distribution of Ni phase, which is included in intermetallide structure. A characteristic feature is that carbon deposition is observed at high temperatures only.

The structure of Ni_3Al before and during catalytic test was examined by *in situ*-XRD, as shown in Fig. 4. Ni_3Al phase was defined at room temperature. No change is observed in the XRD patterns after the reaction till 650 °C. With increasing temperature, the metallic Ni phase becomes detectable at 650 °C and above, implying that the fine Ni particles agglomerate. In addition, Ni_3Al could be destructed partially, supplying Ni phase additionally. Metallic Ni phase and Al–Ni solid solutions become detectable at 750 °C, implying that the system on the base of Ni_3Al reconstructs partially and defects annealing also take place. And, finally, Ni_3Al, NiAl, Al–Ni solid solutions, Ni and $AlNi_3C_{0.5}$ (traces) phases were identified at high reaction temperatures (850–900 °C). Therefore, it is possible to conclude that Ni_3Al underwent the partial destruction during carbon dioxide reforming of methane.

Some substructural characteristics were calculated using Shimadzu XRD-6000 diffractometer. The results are shown in Table 2. As follows from the XRD data, the lattice constant and coherent scattering region increase as the reaction proceeds at 900 °C, formation of Ni_3C or another carbide were not detected, probably, due to short time on stream. Before DRM the content of Ni_3Al and Ni phases were 86.92 and 9.05%, respectively. But after the reaction they became 59.39 and 19.25%. Therefore, it is the evidence that Ni_3Al phase destructs partially, providing Ni phase. In addition, all phases had high lattice constants after DRM in comparison with ideal values, probably, because of the carbon dissolution inside of the intermetallide or Ni crystal lattice.

The surface structure of Ni_3Al catalyst after 24-h reaction was examined using TEM coupled with EDS. Fig. 5 shows the bright field image of the surface after DRM at 900 °C. Some fragments of the surface were covered by the carbon layer with a graphite structure. An increase in the reaction temperature results in the decrease of d_{002} from 0.345 to 0.339 nm (from XRD data) which is close to that of perfect graphite (d_{002} = 0.335 nm). In addition, the average size of filamentous carbon coherent scattering region increases as the reaction temperature elevates. In this study two different types of carbon deposits on the surface of Ni_3Al were observed: (1) graphene which covers large particles of Ni. The size of the globules depends on Ni particles size and varies from 10 to 90 nm and more. The thickness of these carbon layers is 10–15 nm. Therefore, some parts of the surface were deactivated because of the surface covering by graphene layers; (2) carbon filaments (Fig. 6). One carbon filament grows from one catalytic particle, and the graphite planes in filaments are arranged as coaxially cones. The average diameter of carbon filament and the catalyst particle is identical (30–60 nm).

Table 2
Results of powder XRD measurements for catalysts on the base of Ni_3Al.

Phase	Content (vol%)	Real lattice parameter (nm)	Ideal lattice parameter (nm)	Particle diameter (nm)
Before catalytic test in DRM				
Ni_3Al	86.92	0.3578	0.3572	26
NiAl	4.03	0.2889	0.2882	14
Ni	9.05	0.3560	0.3526	90
After catalytic test in DRM				
Ni_3Al	59.39	0.3588	0.3572	42
NiAl	2.83	0.2931	0.2882	13
Ni	19.25	0.3569	0.3526	57
C	8.0	A = 0.2570 c = 0.6893	a = 0.2470 c = 0.6724	62

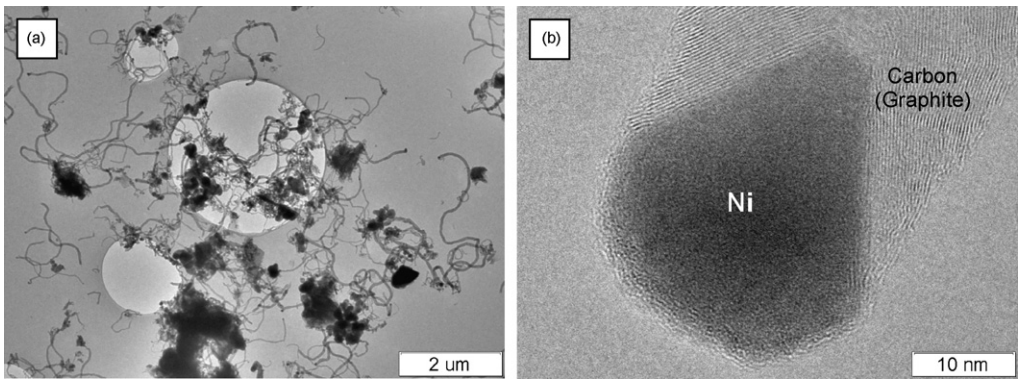

Fig. 6. Morphology of carbon deposits in the Ni_3Al catalyst: general view (a), filament's head with Ni particle (b).

Fig. 7 shows HRTEM analysis after the reaction at the same conditions. Al_2O_3 was observed (position 1) with the parameters close to kappa-Al_2O_3 (No. 52-803 in Crystallographica Search-Match DB) in addition to fine Ni particles 1–2 nm in size; these particles provoked the process of carbon formation on the surface. Only several (5–10) graphene layers formed on that surface. Also the presence of NiO particles in the other catalyst fragments was determined. After the reaction at 900 °C for 24 h, another oxide containing Al and Ni was observed, in addition to Ni, NiO and Al_2O_3. Taking into consideration XPS data (are not presented here) this oxide was identified as $NiAl_2O_4$. For the initial Ni_3Al sample Ni2p can be deconvoluted in three components centered at 852.04, 855.35 and 856.05 eV. These signals can be associated with Ni^0, Ni(II), probably as NiO or $NiAl_2O_4$ due to the asymmetry of the signal, and the third component can be assigned with Ni(II) as well.

The Al2p spectrum showed three chemical states for Al; the signal centred at 71.37 eV associated with the binding energy (BE) to metallic state of Al (Ni_3Al), the second signal localized at 73.96 eV corresponding to Al-oxide (AlOx or Al_2O_3) as amorphous component, the third signal localized at 76.15 eV for possible formation of $NiAl_2O_4$.

After the catalytic tests Ni2p can be deconvoluted in three components centered at 852.54, 855.80 and 857.05 eV. These signals can be associated with Ni^0, Ni(II) probably as NiO or $NiAl_2O_4$ due to the asymmetry of the signal and the third component can be assigned to Ni(II). The Al2s spectrum showed four chemical states of Al; the signal centred at 110.85, 114.25, 118.74 and 120.53 eV. The first signal could be associated tentatively with the shift of BE associated with Ni_3Al, the second signal localized at 114.25 eV corresponding to Al-oxide (AlO_x), the third one at 118.74 eV corresponds to Al_2O_3 as amorphous component and the last component relates to the formation of $NiAl_2O_4$. Thus, we can conclude that Ni^0 oxidized into NiO and $NiAl_2O_4$ (partially, on the surface only) during DRM and Al^0 oxidized into Al_2O_3 (different modifications) and spinel as well. It leads to decrease of catalytic activity and stability in aggressive atmosphere of DRM.

The thermo-gravimetric (TG) and differential thermo-analysis (DTA) of the temperature-programmed oxidation (TPO) in air of the spent catalysts (DRM for 24 at 900 °C) are shown in Fig. 8. The slight weight loss occurring at around 100–200°C was resulted from the evaporation of moisture. However, the carbon deposits over Ni_3Al were oxidized at around 500–800 °C. Meanwhile, two regions with maxima around 590 and 680 °C were identified, which are in consistent with the literature [28]. Fujimoto at al. [28] have designated these peaks as C_α and C_β. First of them, C_α was the active species responsible for the formation of synthesis gas while C_β the most inactive species, was responsible for catalyst deactivation. This indicated that there are two types of carbonaceous species formed on these catalysts. According to TG analysis 6–9% of coke was formed on the surface of Ni_3Al but this catalyst was active and stable enough during 24 h on stream.

The SEM morphologies of Ni_3Al + 5%Mo surface before and after DRM are shown in Fig. 9. The surface is typical for alloy cleavage with some flat areas. After the catalytic tests at temperature 600–900 °C this surface was not significantly changed. Only several parts were covered by carbon deposits in the form of globules. Nevertheless, the other parts of the surface were free of carbon and they were decorated with Ni crystallites (proved by local EDS). In accor-

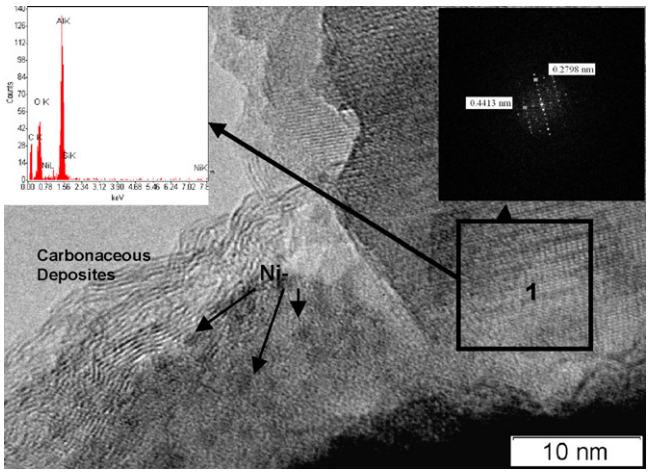

Fig. 7. TEM bright field image of Ni_3Al surface after reaction at 900 °C.

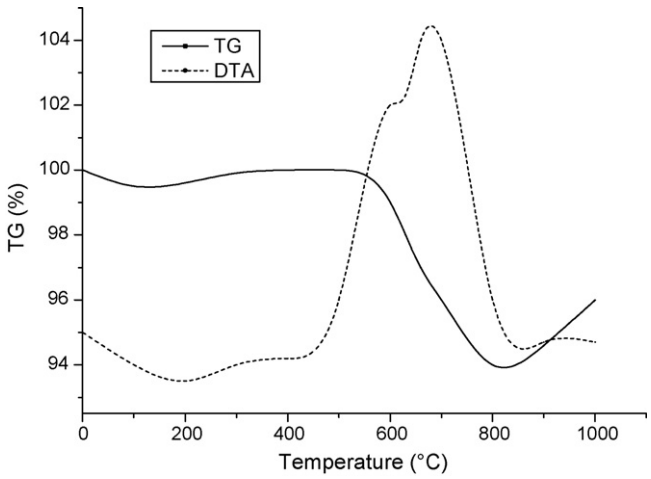

Fig. 8. TG–DSC patterns for Ni_3Al after DRM for 24 h at 900 °C.

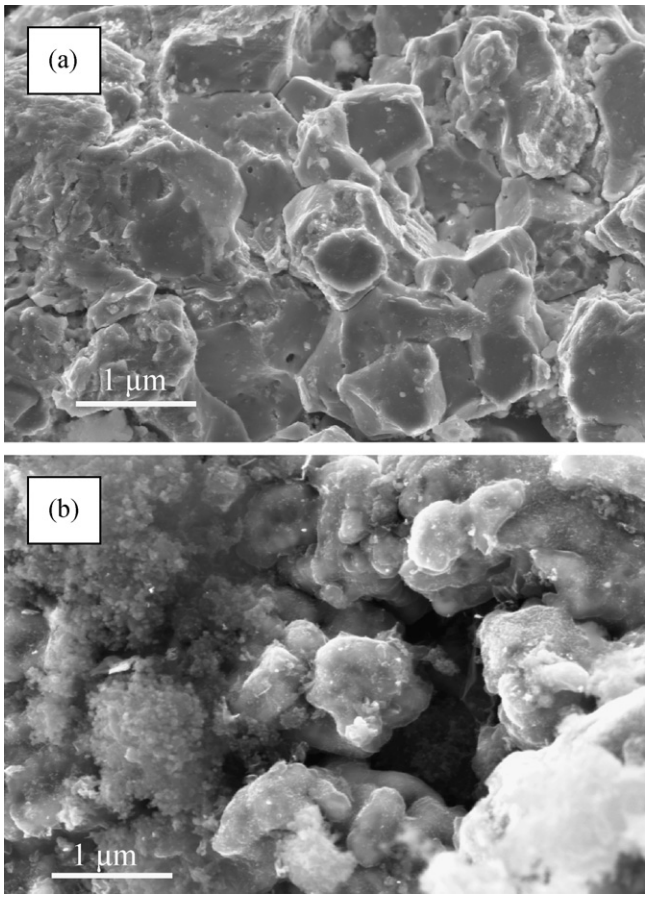

Fig. 9. SEM micrographs of $Ni_3Al + 5\%Mo$ catalysts: (a) initial sample, (b) after DRM. (Time on stream: 24 h, $T = 600–900\,^{\circ}C$, $V(CO_2:CH_4) = 100\,cm^3/min$, $CO_2:CH_4 = 1:1$).

dance with TG–DTA the content of carbon deposition on the surface of catalyst was only 3–5% after 12 h on stream. Ni_3Al, NiAl, Ni, and Mo are the main phases in accordance with XRD (in initial sample). But after DRM we also detected Mo_2C phase and small quantity of carbon (graphite) [30]. Therefore, introduction of small amount of Mo significantly decreases the coking rate and causes an increase in specific activity and a rise in the catalysts resistance to coking. These data are in consistent with the literature [29]. If the decrease of coking rate of $Ni_3Al + 5\%Mo$ catalysts is not caused by acceleration of the filamentous deposit gasification but by a decrease of a number of coking crystallites, then the reason for the observed effect can be found in the following—a reduction of carbon solubility in the crystallite due to formation of the Ni–Mo alloy which makes it difficult to create proper conditions for filamentous carbon formation.

The studies of $Ni_3Al + 5\%Mo$ catalyst by HRTEM showed formation of NiMo intermetallide (Fig. 10). The driving force for carbon diffusion and for the global process of carbon filament formation is the difference in solubility at the gas/metal interface and the carbon filament/metal interface. According to the model proposed by Snoeck et al. [35], the nucleation of filamentous carbon is caused by the formation of a solution of carbon in nickel that is supersaturated with respect to filamentous carbon. The degree of supersaturation is determined by the affinity for carbon formation of the gas phase. However, the solubility of carbon in nickel is lowered by the presence of additives (such as Mo) in its lattice and the supersaturation necessary for whisker-like carbon filaments cannot be attained." The improvement of the reforming performance can be attributed to the formation of two-dimensional surface defects and dislocations as well.

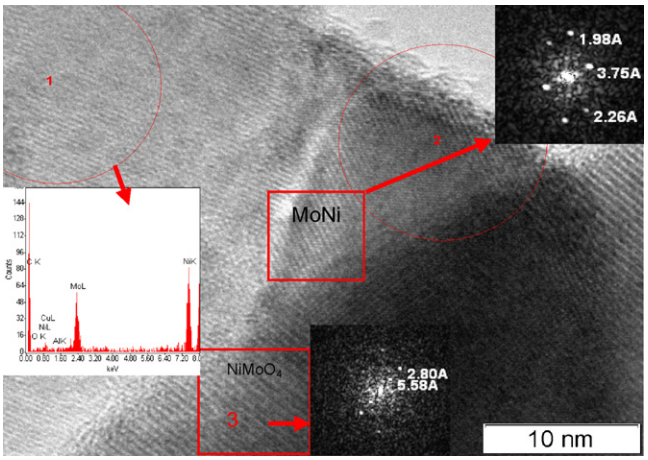

Fig. 10. HRTEM bright field image of $Ni_3Al + 5\%Mo$ surface after DRM for 24 h at 900 °C. EDS spectra taken from position 1, showing the presence of NiMo, Fourier diffraction patterns taken from positions 2 and 3, showing the formation MoNi and $NiMoO_4$ compounds on the catalyst surface.

4. Conclusion

This work shows that Ni_3Al and $Ni_3Al + 5\%Mo$ are the promising catalysts for the process of carbon dioxide reforming of methane. Ni_3Al undergoes the partial deactivation because of the Ni sintering and carbon formation. There are two types of carbon deposition on the Ni_3Al surface formed in DRM: graphene and filaments. Nevertheless, Ni_3Al serves as a support due to some appropriate properties, such as high thermoresistance; high stability and mechanical tics; and high thermal conductivity. In addition, Ni_3Al, despite negligible destruction, is able to supply pure Ni particles which are active in DRM.

Mo, as a promoter, improves the catalytic activity and stability of Ni_3Al intermetallide catalyst. The carbon deposition content on $Ni_3Al + 5\%Mo$ surface is twice as little as on Ni_3Al. The observed effects of the Mo presence result from overlapping of a few phenomena:

1. Formation of Mo_2C phase during the process of carbon dioxide reforming of methane which is very active and stable in DRM.
2. Formation of alloy Ni–Mo and reduction of carbon solubility.
3. Reduction of dehydrogenation degree of dissociating hydrocarbon fragments.

Acknowledgements

The author of the article acknowledges Dr. Yu.S. Naiborodenko, N.G. Kasatsky for the help in catalyst synthesis by SHS, Dr. A.N. Shmakov and M.R. Sharafutdinov for the mutual work in VEPP-3 station of Siberian Synchrotron and Terahertz Radiation Center of Budker Institute of Nuclear Physics of SB RAS, Dr. V.I. Zaikovskii for HRTEM studies and Prof. L.A. Arrebola for XPS data.

References

[1] J. Zhang, H. Wang, A.K. Dalai, Appl. Catal. A: Gen. 339 (2008) 121.
[2] C. Song, A.M. Gaffney, K. Fujimoto, Proc. ACS Symp. Ser., American Chemical Society, Washington, DC, 2002.
[3] (a) M.M. Halmann, M. Steinberg, Greenhouse Gas Carbon Dioxide Mitigation: Science and Technology, Lewis Publishers, Boca Raton, FL, 1999; (b) H. Gunardson, Industrial Gases in Petrochemical Processing, Marcel Dekker, New York, 1998.
[4] M.C. Bradford, M.A. Vannice, J. Catal. 173 (1998) 157.
[5] T. Inui, K. Saigo, Y. Fujii, K. Fukioka, Catal. Today 26 (1995) 295.
[6] J.-Y. Ren, W. Qin, F.N. Egolfopoulos, H. Mak, T.T. Tsotsis, Chem. Eng. Sci. 56 (2001) 1541–1549.
[7] M. Bradford, M. Vannice, Catal. Rev. Sci. Eng. 41 (1999) 1.

[8] A. Lewicki, T. Paryjczak, W.K. Jozwiak, J.M. Rynkowski, Wiad. Chem. 56 (2002) 279.
[9] K. Seshan, J.A. Lercher, Proceedings of the International Symposium on CO_2, Hemavan, Sweden, September 20–24, 1993, The Royal Society of Chemistry, Cambridge, 1994, p. 16.
[10] J.T. Richardson, S.A. Paripatyadar, Appl. Catal. 61 (1990) 293.
[11] T. Kodama, T. Shimizu, T. Kitayama, Energy Fuels 15 (2001) 69.
[12] T. Kodama, T. Shimizu, K.I. Shimizu, T. Kitayama, Energy Fuels 16 (2002) 1016.
[13] M. Yang, H. Papp, Catal. Today 115 (2006) 199–204.
[14] J.H. Bitter, K. Seshan, J.A. Lercher, J. Catal. 171 (1997) 279.
[15] A.N.J. van Keulen, M.E.S. Hegarty, J.R.H. Ross, P.F. van den Oosterkamp, Stud. Surf. Sci. Catal. 107 (1997) 537.
[16] M.M.V.M. Souza, D.A.G. Aranda, M. Schmal, J. Catal. 204 (2001) 498.
[17] V.R. Choudhary, B.S. Uphade, A.S. Mamman, Catal. Lett. 32 (1995) 387.
[18] V.R. Choudhary, B.S. Uphade, A.S. Mamman, Appl. Catal. A 168 (1998) 33.
[19] J.Y. Mehr, K.J. Jozani, A.N. Pour, Y. Zamani, React. Kinet. Catal. Lett. 75 (2002) 267.
[20] T. Horiuchi, K. Sakuma, T. Fukui, Y. Kubo, T. Osaki, T. Mori, Appl. Catal. A 144 (1996) 111.
[21] Z.L. Zhang, X.E. Verykios, Catal. Today 21 (1994) 589.
[22] J.R. Rostrub-Nielsen, in: J.R. Anderson, M. Boudard (Eds.), Catalysis: Science and Technology, vol. 5, Springer, Berlin, 1984, pp. 1–117.
[23] E. Tracz, R. Scholz, T. Borowiecki, Appl. Catal. 66 (1) (1990) 133.
[24] J.B. Claridge, A.P.E. York, A.J. Brungs, C. Marquez-Alvarez, J. Sloan, S.C. Tsang, M.L.H. Green, J. Catal. 180 (1998) 85.
[25] Z. Xu, M. Zhen, Y. Bi, K. Zhen, Appl. Catal. A 198 (2000) 267.
[26] J.R. Rostrub-Nielsen, J.H. Bak-Hansen, J. Catal. 144 (1993) 38.
[27] A. Shamsi, Ch.D. Johnson, Catal. Today 84 (2003) 17.
[28] Y.-G. Chen, K. Tomishige, K. Fujimoto, Appl. Catal. A 161 (1997) L11.
[29] L. Kepinski, B. Stasinska, T. Borowiecki, Carbon 38 (2000) 1845.
[30] L.V. Galaktionova, L.A. Arkatova, L.N. Kurina, T.S. Kharlamova, Yu.S. Naiborodenko, N.G. Kasatsky, N.N. Golobokov, Russ. J. Phys. Chem. A 81 (10) (2007) 1718.
[31] L.A. Arkatova, L.N. Kurina, L.V. Galaktionova, Russ. J. Phys. Chem. A 83 (4) (2009) 624.
[32] G. Xanthopoulou, G. Vekinis, Appl. Catal. B 19 (1998) 37.
[33] Y. Ma, Y. Xu, M. Demura, T. Hirano, Appl. Catal. B 80 (2007) 15.
[34] Y. Li, Y. Wang, X. Zhang, Z. Mi, Int. J. Hydrogen Energy 33 (2008) 2507.
[35] J.W. Snoeck, G.F. Froment, M. Fowles, J. Catal. 169 (1) (1997) 240.
[36] V.I. Itin, Yu.S. Naiborodenko, Self-propagating High-temperature Synthesis of Intermetallic Compounds, TSU, Tomsk, 1989, p. 214.